

# BUCKLING REDUCTION FACTORS FOR STAINLESS STEEL SHELL STRUCTURES

K. T. Hautala  
Consulting KORTES Ltd., Finland

Copyright © 2003 The Steel Construction Institute

## Abstract

*The material behaviour of stainless steel strongly differs from that of mild steel beyond the proportional limit. Consequently, the buckling behaviour of mild steel structures and stainless steel structures will differ from each other in so far as for any given stainless steel structure of medium slenderness, i.e. belonging to the 'elastic-plastic' region, the buckling capacity is lower than for a comparable mild steel structure of identical shape and area.*

*This paper shows numerical buckling reduction factors for stainless steel shell structures. Firstly some buckling strength curves of European standards are numerically reproduced using simple substitute imperfections. Proposals are then made for modification of standards in order to include stainless steels. Preliminary new proposals are made for modelling of material behaviour of stainless steels and buckling design of shell structures under meridional compression.*

## 1 INTRODUCTION

Most of the strength reduction formulations adopted in standards are empirically based, making it difficult to extend them without major experimental studies. However, if theoretical calculations are to be used to extend design rules to new cases, the existing design rules have to be first reproduced using theoretical calculations.

It is well known that, when aiming at realistic calculated buckling strengths of real shells, it is necessary to include the imperfections into the numerical model. Many publications have been written about the form of imperfection that should be used in calculations of the buckling strength of cylinders that have not yet been constructed. The imperfections should have the dual attributes of realism in practical constructions and severity in their effect on the buckling strength [12].

The three main groups of imperfections are - geometrical (out-of-straightness, initial ovality and geometrical eccentricities, for example), structural (residual stresses and material inhomogenities) and loading imperfections (non-uniform edge load distribution, unintended edge moments, load eccentricities and load misalignments as well as imperfect boundary conditions). Also the constructional defects, such as small holes, cut outs, rigid inclusions and delaminations, could be counted as structural imperfections. The geometrical imperfections are most frequently used in the shell buckling computations and they also serve as a substitute for any other kind of imperfection because of the simplicity in specifying them.

The worst currently known geometrical imperfections are generally similar to the classical buckling waveforms or to the ones in the Euler mode. However, these modes are mostly far from practical. According to many authors, imperfection data banks should be established in order to obtain more accurate predictions of the buckling loads of shells. If extensive data were accumulated there would be a chance of obtaining a meaningful correlation between the manufacturing processes and the imperfections, which would permit a design for an expected imperfection shape and magnitude. An extensive summary of state of knowledge is given in [7].

Anyway, especially for civil and mechanical engineering structures, very few imperfection measurements are known. One reason for this is that the measuring of imperfections on full-scale structures is rather expensive, and it can effectively be done only on industrially mass-produced structures. However, many civil engineering structures are made in a small numbers or as one off samples. Furthermore, many structures, such as storage tanks, containers, pipelines, silos and off-shore structures are field assembled structures, and this involves a great scatter in the imperfection pattern, which cannot easily be monitored during construction. Moreover, the imperfection pattern can also change during the lifetime of the structure,

which usually happens as a consequence of the daily wearing, or even as a result of accidental causes [10].

No matter how sophisticated a numerical imitation of an imperfection field may be, it still represents merely a 'substitute imperfection' because certain components of the imperfections are not included and must therefore be 'substituted' in the imperfection model.

With this in mind, it makes sense to use extensive parametric studies and the simplest possible substitute imperfection model. After a series of pilot studies [7,8] a single axisymmetric inward substitute imperfection with a sinusoidal meridional shape of amplitude  $w_0$  and wavelength  $1.73\sqrt{rt}$  located in the middle of the cylinder length was chosen, where  $r$  is the cylinder radius and  $t$  is the cylinder wall thickness.

## 2 NUMERICAL REPRODUCTION OF STANDARDS

The basic idea is to calculate directly the buckling strength difference caused by the non-linear stress-strain relationship of austenitic stainless steels compared to the ideally elastic-plastic one of structural steels. For that purpose, a numerical imperfection model has to be established and calibrated against codified characteristic buckling curves for shells made of structural steel.

The calibration yielded a substitute imperfection amplitude  $w_0/r = 1/500$  (independent of the shell slenderness) to be appropriate in order to reproduce numerically the buckling design curve of ECCS-Recommendations (see Fig. 1). A constant ratio  $w_0/r$  means, in fact, an increasing normalised imperfection amplitude  $w_0/t$  with increasing  $\lambda$  or  $r/t$ . This is a well-known characteristic of real shells [7].

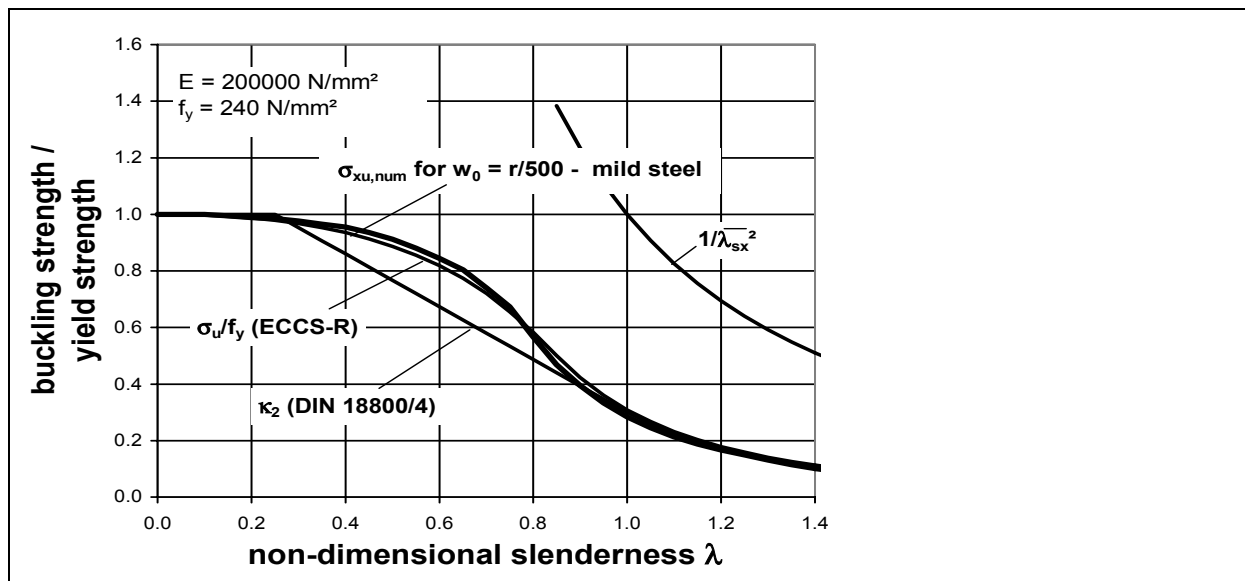


**Figure 1** Numerical buckling curve for  $w_0 = r/500$  (mild steel), compared to the characteristic buckling curves acc. to ECCS-R and DIN 18800-4.

Fig. 2 shows the numerical elastic-plastic buckling strength curves that reproduce the design curves of ENV 1993-1-6. Using a single imperfection with amplitude that strongly varies with  $r/t$ -ratio could only reproduce these design curves. The class B curve was reproduced by using six different amplitudes between  $w_0 = r/170$  and  $w_0 = r/400$ , for example.

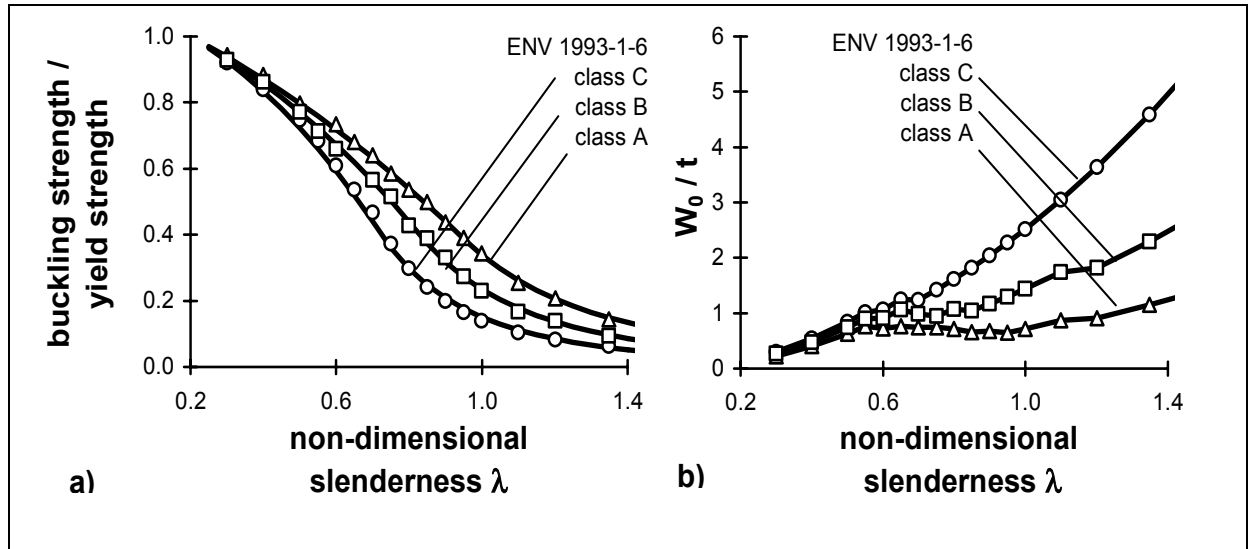


**Figure 2** a) Numerically reproduced buckling design curves (mild steel) of ENV 1993-1-6, b) the corresponding numerical imperfection amplitudes.

### 3 NUMERICAL BUCKLING CURVES FOR STAINLESS STEELS

In the next phase the pair of computer runs have to be performed for every given shell and material parameter combination, firstly using the bilinear elastic-plastic material model and secondly using the strain hardening Ramberg-Osgood material model. Each of them delivers a ratio of a Ramberg-Osgood buckling load over the elastic-plastic load. These ratios may now be treated as material buckling correction factors of a material following the Ramberg-Osgood material model for which the initial elastic modulus  $E_0$  and the 0.2% proof stress  $R_{p0.2}$  are taken as being  $E$  and  $f_y$  in the sense of structural steel. The correction factors proposed in [9,13,14] are summarized in Table 1.

**Table 1** Buckling reduction factors for stainless steels.

Temperature $T \leq 100^\circ\text{C}$ :			Temperature $T > 100^\circ\text{C}$ :		
$\Psi = 1.00$	if	$\bar{\lambda} \leq 0.40$	$\Psi = 1.00$	if	$\bar{\lambda} \leq 0.30$
$= 1.00 - 0.800 (\bar{\lambda} - 0.40)$	if	$0.40 < \bar{\lambda} < 0.65$	$= 1.00 - 0.714 (\bar{\lambda} - 0.30)$	if	$0.30 < \bar{\lambda} < 0.65$
$= 0.80$	if	$0.65 \leq \bar{\lambda} \leq 0.80$	$= 0.75$	if	$0.65 \leq \bar{\lambda} \leq 0.80$
$= 0.80 + 1.000 (\bar{\lambda} - 0.80)$	if	$0.80 < \bar{\lambda} < 1.00$	$= 0.75 + 0.833 (\bar{\lambda} - 0.80)$	if	$0.80 < \bar{\lambda} < 1.10$
$= 1.00$	if	$1.00 \leq \bar{\lambda}$	$= 1.00$	if	$1.10 \leq \bar{\lambda}$

In the table  $\Psi$  = buckling reduction factor and  $\bar{\lambda}$  = non-dimensional slenderness.

The validity of the above given numerical material buckling reduction factors has been verified for the three quality classes of ENV 1993-1-6 in Fig. 3a. The discontinuous nature of the curves results from the fact that for different slenderness different imperfection amplitudes have been used, that has been varied stepwise rather than gradually.

The above discussed numerical analysis was based on material properties of  $E = 200 \text{ GPa}$ ,  $f_y = 240 \text{ N/mm}^2$ ,  $n = 6.0$ . The Fig. 3b verifies the validity of the equations given in table 1 for the strength classes of 220, 240 and 290 of ENV 1993-1-4, as well.

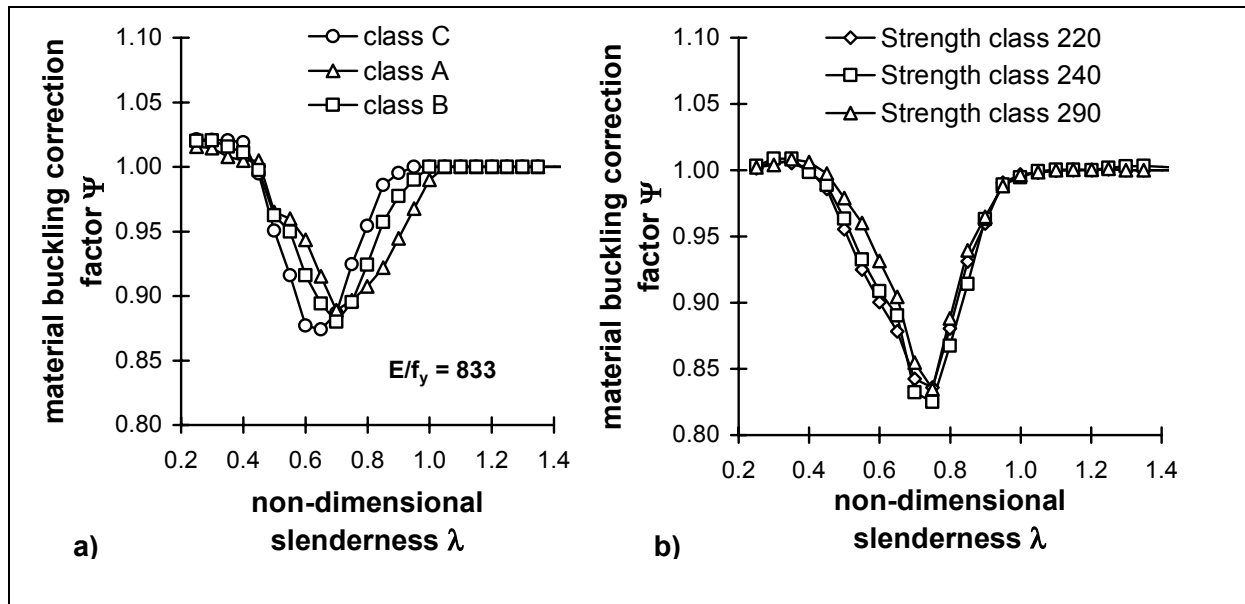


**Figure 3** Numerical material buckling correction factors for a) quality classes of A, B and C of ENV 1993-1-6 and b) strength classes of 220, 240 and 290 of ENV 1993-1-4.

The above given material buckling correction factors may be rather conservative when the real proportional limit of austenitic stainless steel is a lot higher and the real stress-strain curve is less rounded than assumed in codes. According to the experimental results of Hautala and Schmidt [8] the material behaviour of stainless steels may be modelled using the Ramberg-Osgood formulation up to 2% strain values (see Fig. 4.)

$$\varepsilon = \sigma/E + 0.002 (\sigma/f_y)^n ; \quad n = \log (\varepsilon_1/\varepsilon_2) / \log (\sigma_1/\sigma_2)$$

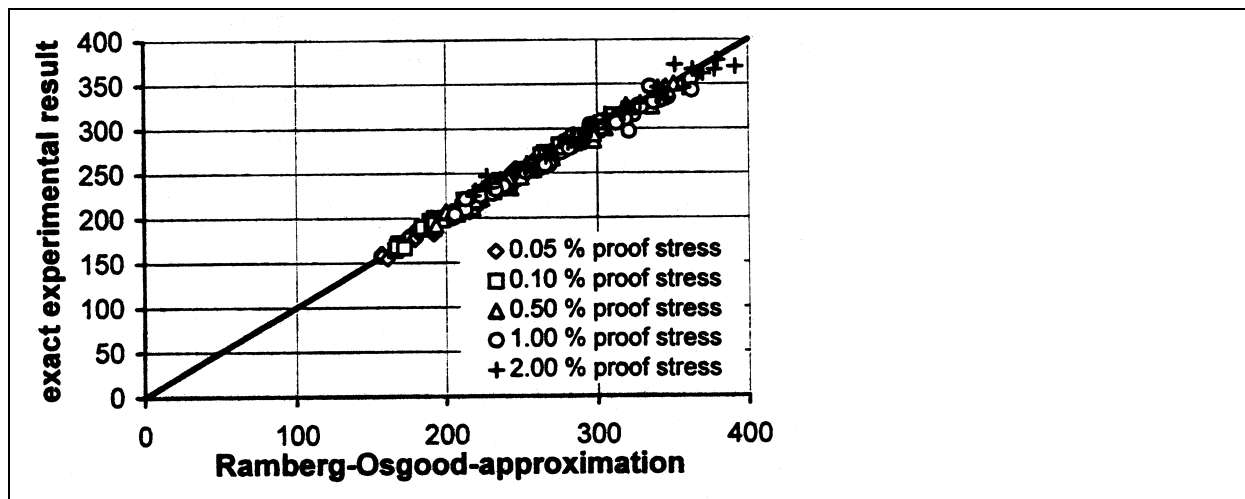


**Figure 4** Correlation between real material behaviour and Ramberg-Osgood approximation [7].

However, the measured exponents  $n$  of the Ramberg-Osgood material model exceeded the codified values of ENV 1993-1-4 ( $n = 6.0$  for X6CrNiMoTi17-12-2 at 20°C) obviously. One typical factor registered in the experiments was  $n = 12$ , but also values up to  $n = 16$  were measured. Fig. 5 shows the influence of the exponent  $n$  on the numerical buckling curve. For  $n = 12$  the buckling curve is at its most 10% above the curve for  $n = 6$ , when  $\lambda = 0.55$ -1.0.

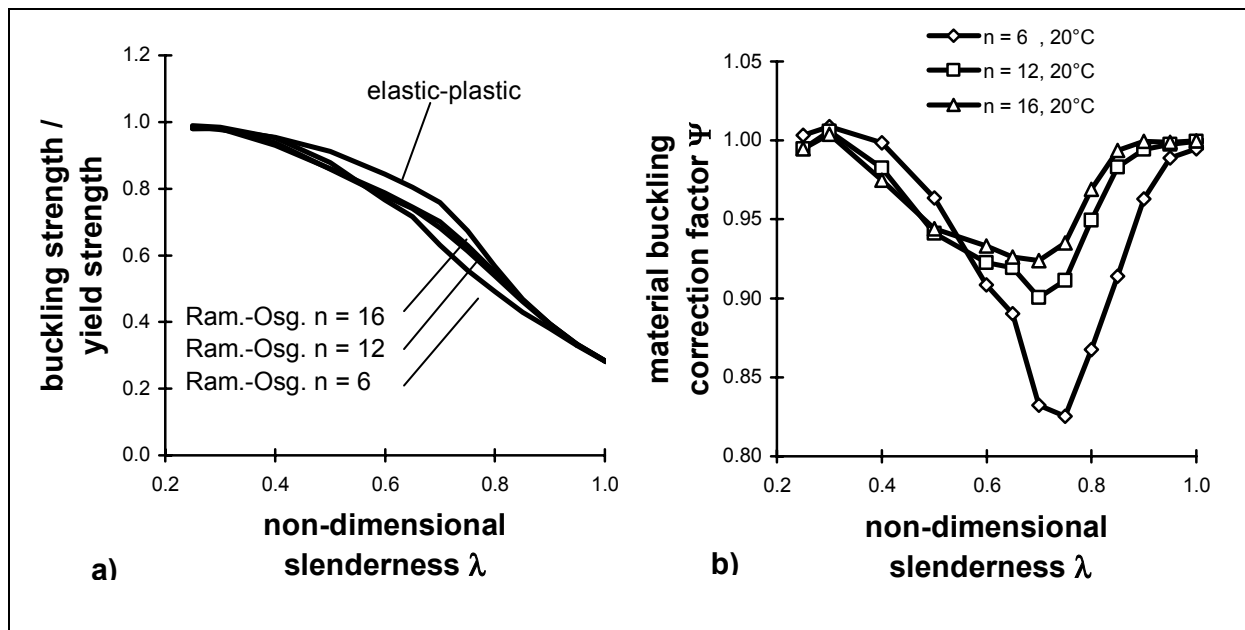


**Figure 5** Numerical buckling curves and material buckling correction factors for different n-exponents of the Ramberg-Osgood material model.

However, the smaller material buckling reductions resulting from the higher n-values can be applied only if the real material properties are experimentally verified. The practical buckling analysis has to be based on n-exponents given in codes as long as no further information is available.

## 4 VERIFICATION OF THE BUCKLING REDUCTION FACTORS

The basic idea is to supplement the modern buckling codes to include stainless steels by adding a material buckling correction factor to the existing design procedure without further changes of the codes. The actual buckling design stresses would be simply multiplied by this factor in order to take all the relevant influences resulting from the use of stainless steel into account.

In order to verify the applicability of the proposed buckling reduction factors, some experimental results are compared with current codes first using the current characteristic design values, and then using the improved characteristic design values. This kind of presentation shows directly whether the codes are giving safe, exact or unsafe estimations when compared with the experiments.

### 4.1 ECCS-Recommendations (Fig. 6)

It has been found reasonable to compare the experimental results to the lower bound curves representing the physical background of different codes. Thus, the calculation has been carried out without the additional partial safety factor  $\gamma = 4/3$ . Of course, the measured material properties and geometry have been applied.

It is obvious from Fig. 6a that ECCS-R gives unsafe results for most of the cylinders. Thus it is clear that the design procedure of ECCS-R has to be supplemented to include stainless steels. As Fig. 6b demonstrates this can be done by using the material buckling reduction factors for stainless steels. The fact that some of the experimental results are still slightly on the unconservative side has to do with a known principal shortcoming of the ECCS-curve for medium-thick cylinders.

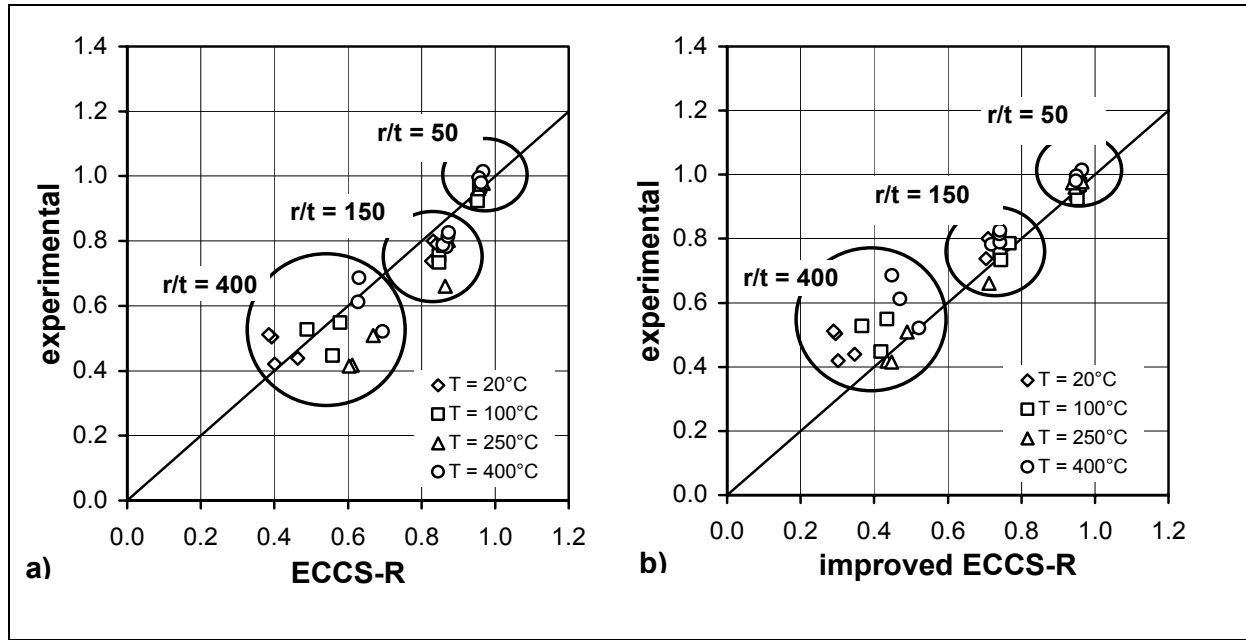


**Figure 6** a) Checking of ECCS-R with the help of relative experimental buckling stresses, b) effect of the proposed correction on the relative buckling stresses acc. to ECCS-R.

#### 4.2 ENV 1993-1-6 (Fig. 7)

In ENV 1993-1-6 the meridional elastic imperfection factor  $\alpha_x$  does not directly correspond to the lower bound of experimental results. That is why the experimental results are here compared to calculated values determined by using a 4/3-fold imperfection factor of

$$\alpha_x = 0.83 / (1 + 1.91(w/t)^{1.44})$$

In the quality class B the direct use of ENV 1993-1-6 yields unsafe predictions for most of the cylinders with  $r/t = 400$  and  $150$ . For the cylinders with  $r/t = 50$  the results are quite satisfactory. The predictions in the quality class A are somewhat worse and in the quality class C somewhat better, respectively. The use of the buckling reduction factors for stainless steels yields satisfactory results for all of the cylinders.

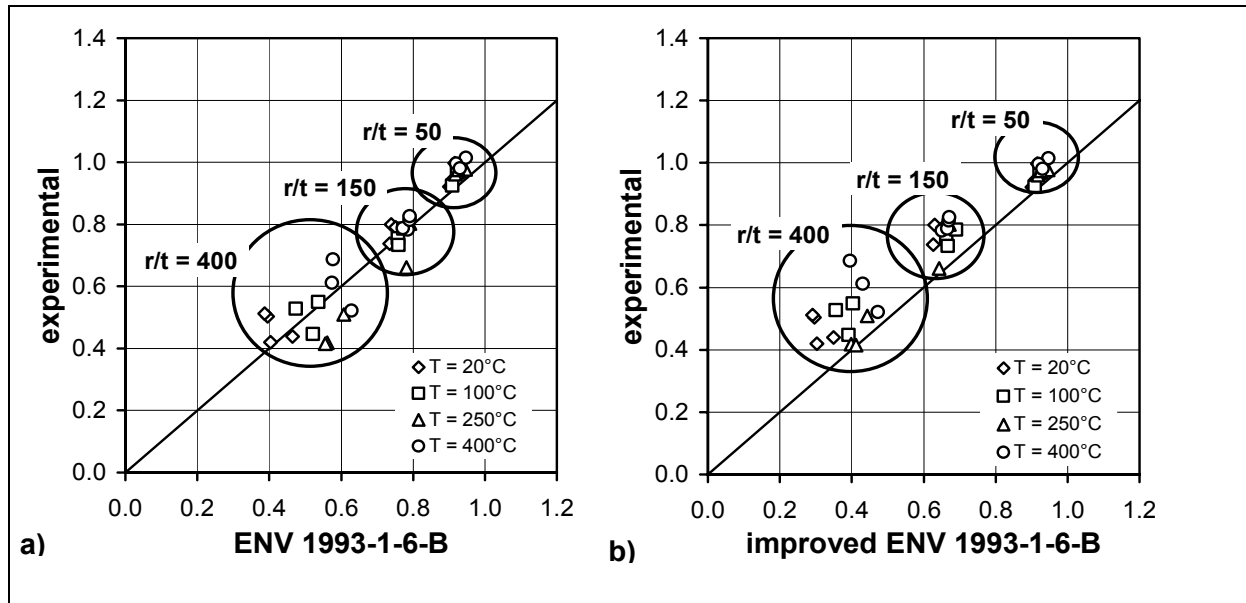


**Figure 7** a) Checking of ENV 1993-1-6 class B with the help of relative experimental buckling stresses, b) effect of the proposed correction on the relative buckling stresses acc. to ENV 1993-1-6.

#### 4.3 DIN 18800-4 (Fig. 7)

The results of DIN 18800-4 correspond to those of ENV 1993-1-6, quality class B.

#### 4.4 DIN 4133 in combination with DIN 18800-4 (Fig. 8a)

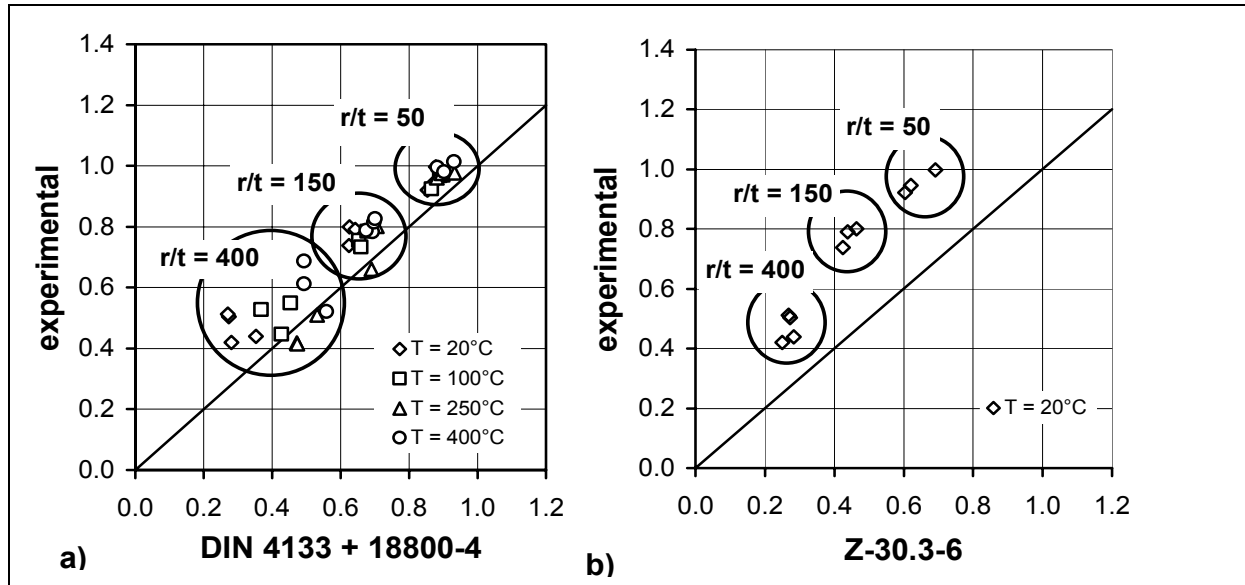


**Figure 8** Checking of a) DIN 4133 in combination with DIN 18800-4 and b) the Technical Approval Z-30.3-6 with the help of relative experimental buckling stresses.

The buckling analysis is here to be carried out in accordance with DIN 18800-4, except that now the fictitious reduced elastic modulus  $E = 170$  GPa at  $20^\circ\text{C}$  is to be used instead of  $E = 200$  GPa. Correspondingly, the fictitious values of  $E$  at elevated temperatures are 164 GPa ( $100^\circ\text{C}$ ), 153 GPa ( $250^\circ\text{C}$ ) and 142 GPa ( $400^\circ\text{C}$ ).

On the basis of this comparison it is clear that the use of the fictitious values of elastic modulus in connection with the measured values of  $f_y$  gives slightly conservative predictions for cylinders with  $r/t = 50$  and 150 and slightly unconservative predictions for cylinders with  $r/t = 400$ .

Instead of modifying the design procedure of DIN 4133, it is recommended to use, the modified ENV 1993-1-6, ECCS-R or DIN 18800-4.

#### 4.5 Z-30.3-6 Technical Approval for Stainless Steels (Fig. 8b)

The buckling analysis is here to be carried out in accordance with DIN 18800-4, as well, except that now the secant modulus  $E_{\text{sek}}$  is to be used instead of  $E$ . The secant modulus  $E_{\text{sek}}$  is to be calculated using a reduced fictitious value of elastic modulus  $E = 170$  GPa. Z-30.3-6 is valid only at ambient temperature. That is why only the experimental results at  $20^\circ\text{C}$  are given in Fig. 8b.

The design procedure of Z-30.3-6 yields very conservative predictions for all of the cylinders. Instead of modifying the design procedure of Z-30.3-6, it is recommended to use, the modified ENV 1993-1-6, ECCS-R or DIN 18800-4.

## 5 CONCLUSIONS

On the basis of the comparison between the experimental buckling stresses and the characteristic design values of ECCS-R, ENV 1993-1-6 and DIN 18800-4, it is obvious that these codes have to be modified to enable inclusion of stainless steels. Applying a material buckling correction factor to the actual design procedures without any further changing of the design methods can do this.

This method has the advantage over the use of fictitious elastic moduli in that now the reduced buckling capacity of stainless steel cylinders in the slenderness region of  $\lambda = 0.3$ -1.0 can be directly taken into

account without affecting the buckling load predictions for cylinders with other slenderness. All in all, the use of fictitious reduced elastic modulus, such as in DIN 4133 and technical approval Z-30. 3-6 seems to be over conservative. Even the proposal in [11] to use a fictitious elastic modulus  $E = 1000 \cdot f_y$  in combination with DIN 18800-4 when designing materials with  $E/f_y > 1000$  seems to be much too conservative on the basis of experimental results.

The material buckling correction factors that are given in Table 1 are recommended for general use when designing cylindrical shell structures made of austenitic stainless steels under a uniform temperature action in the range of 20-500°C.

## 6 REFERENCES

- [1] DIN 4133 – Schornsteine aus Stahl. Berlin: Beuth Verlag, 1991.
- [2] DIN 18800 –4 – Stahlbauten: Stabilitätsfälle, Schalenbeulen. Berlin; Beuth Verlag. 1990.
- [3] ECCS – Recommendations: Buckling of Steel Shells, 4<sup>th</sup> ed. Brüssel: ECCS Secretariat. 1998.
- [4] ENV 1993-1-4 – Design of Steel Structures, Supplementary Rules for Stainless Steels. Brüssel CEN. 1996.
- [5] ENV 1993-1-6 – Design of Steel Structures, Supplementary Rules for Shell Structures. Brüssel CEN. 1999.
- [6] Z-30.3-6 - Allgemeine bauaufsichtliche Zulassung – Bauteile und Verbindungselemente aus nichtrostenden Stählen. Berlin: Deutsches Inst. für Bautechnik. 1998.
- [7] Hautala, K. T., Buckling of Axially Compressed Cylindrical Shells Made of Austenitic Stainless Steels under Ambient and Elevated Temperatures. Diss. Universität Essen, FB10 - Stahlbau. 1998.
- [8] Hautala, K. T.; Schmidt, H., Buckling Tests on Axially Compressed Cylindrical Shells of Various Austenitic Stainless Steels at Ambient and Elevated Temperatures. Bericht 76, Universität Essen, FB10. 1998.
- [9] Hautala, K. T.; Schmidt, H., Buckling of Axially Compressed Cylindrical Shells made of Austenitic Stainless Steel at Ambient and Elevated Temperatures. Lightweight Steel and Aluminium Structures. Ed. Mäkeläinen; Hassinen. Elsevier Science Ltd, pp. 233-240. 1999.
- [10] Knoedel, P.; Ummenhofer, T., Substitute Imperfections for the Prediction of Buckling Loads in Shell Design. CA-Silo. WG3: Metal Silo Structures, Imperfections in Metal Silos, Measurement, Characterisation and Strength Analysis. Workshop held at INSA Lyon, pp. 87-101. 1996.
- [11] Lindner, J., Scheer, J., Schmidt, H., Beuth-Commentar Stahlbauten – Erläuterungen zu DIN 18800 Teil 1 bis 4, 3. Auflage. Berlin: Beuth Verlag. 1998.
- [12] Rotter, J. M., Design Standards and Calculations for Imperfect Pressurised Axially Compressed Cylinders. Int. Conf. Carrying Capacity of Steel Shell Structures, Brno, pp. 354-360. 1997.
- [13] Schmidt, H.; Hautala, K. T., Beulsicherheit schalenartiger Stahlkonstruktionen aus austenitischen Stählen bei erhöhten Temperaturen am Beispiel axialgedrückter Kreiszyinderschalen. Bericht FV DIBt IV 1-5-873/98. Universität Essen, FB10 – Stahlbau. 2000.
- [14] Schmidt, H., Stahlbau-Kalender 2002, Stahlbaunormen, Beulsicherheitsnachweise für Schalen nach DIN 18800 Teil 4, E-DAST-Richtlinie 017 und DIN V ENV 1993-1-6. Ernst & Sohn. 2002.